Dynamic Roughening of Directed Lines

Deniz Ertaş and Mehran Kardar

Department of Physics, Massachusetts Institute of Technology, Cambridge, Massachusetts 02139

(Received 1 May 1992)

We study the fluctuations of a stretched string, e.g., a vortex line, moving in a random medium. A pair of nonlinear equations are proposed to describe the evolution of longitudinal and transverse coordinates. The dynamic scaling of the fluctuations is studied analytically (by renormalization group) and numerically. In most cases the fluctuations are superdiffusive, governed by a dynamic exponent $z = \frac{3}{2}$.

In the past few years, a combination of numerical and analytical studies has greatly advanced our understanding of dynamic fluctuations of growing interfaces [1]. The evolution of the surface profile by addition of particles is a prototype of problems in open and nonequilibrium systems where the traditional approach of near equilibrium statistical mechanics is difficult to apply. Alternatively, one can regard the evolution equations as more fundamental, and proceed by constructing the most general equations consistent with the symmetries and conservation laws of the situation under study [2]. Here we apply such an approach to the motion of a string, e.g., a dislocation, polymer, or a vortex line, and construct the simplest *local,* nonlinear approximation for the dynamics of its fluctuations. The nonlinearities generated by the overall drift of the line are relevant and change the scaling of the fluctuations from the equilibrium form. In particular, in most cases the dynamics is superdiffusive, characterized by an exponent $z = \frac{3}{2}$.

Consider a vortex line in a superconductor with randomly distributed impurities. It will be stretched along the direction of the external magnetic field, and for small driving forces pinned by the impurities. A sufficiently strong force, however, unpins the line and causes a drift along the current direction. The impurities now appear as weak barriers that deflect portions of the vortex line without impeding its overall drift. We address the dynamics of fluctuations caused by such weak impurities on the *unpinned* line. When stationary, all directions perpendicular to a stretched line are equivalent in an isotropic material. By contrast, for a moving line fluctuations parallel and perpendicular to the average velocity need not be similar. These "longitudinal" and "transverse" fluctuations are denoted respectively by $h_\parallel(x)$ and $h_\perp(x)$, where x labels the axis along which the line is stretched, as shown in Fig. 1. The time evolution of a dense collection of such lines has been studied by Hwa [3]. Here we examine the dilute limit and the fluctuations of a single line.

The average drift velocity v breaks the symmetry between forward and backward motions and allows introduction of nonlinearities in the equations of motion [2,4]. Assuming that the evolution of the line is *dissipative* and

local, the simplest such equations are

$$\partial_t h_\parallel = v_\parallel \partial_x^2 h_\parallel + \frac{\lambda_\parallel}{2}(\partial_x h_\parallel)^2 + \frac{\lambda_\times}{2}(\partial_x h_\perp)^2 + \eta_\parallel(x,t),$$

$$\partial_t h_\perp = v_\perp \partial_x^2 h_\perp + \lambda_\perp \partial_x h_\parallel \partial_x h_\perp + \eta_\perp(x,t). \tag{1}$$

The randomly distributed impurities are the origin of the noise terms $\eta_\parallel(x,t)$ and $\eta_\perp(x,t)$. Since $h_\parallel$ and $h_\perp$ represent fluctuations around the mean, the average of η_α is zero, while

$$\langle \eta_\parallel(x,t)\eta_\parallel(x',t')\rangle = 2D_\parallel \delta(x-x')\delta(t-t'),$$

$$\langle \eta_\perp(x,t)\eta_\perp(x',t')\rangle = 2D_\perp \delta(x-x')\delta(t-t'). \tag{2}$$

Nontrivial correlations or non-Gaussian distributions of the noise, which may potentially alter the scaling behavior [5,6], are not considered in this paper. In the absence of transverse fluctuations, Eq. (1) describes a growing surface [7], and is intimately linked to the randomly stirred Burgers equation [8,9]. One way to obtain these equations is to generalize to an n-dimensional space of fluctuations h_α. The drift velocity v_α selects a direction in this n-dimensional space, and by contracting up to two derivatives of h, we can construct the evolution equation
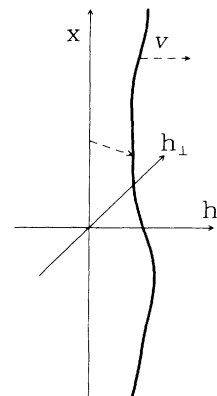

FIG. 1. Longitudinal, $h_\parallel$, and transverse, $h_\perp$, fluctuations of a line stretched in a direction perpendicular to its average velocity v.

$$\partial_t h_\alpha = [\nu_1 \delta_{\alpha,\beta} + \nu_2 v_\alpha v_\beta] \partial_x^2 h_\beta + [\mu_1(\delta_{\alpha,\beta}v_\gamma + \delta_{\alpha,\gamma}v_\beta) + \mu_2 v_\alpha \delta_{\beta,\gamma} + \mu_3 v_\alpha v_\beta v_\gamma] \frac{\partial_x h_\beta \partial_x h_\gamma}{2} + \eta_\alpha. \tag{3}$$

It is easy to establish the equivalence of Eqs. (1) and (3) and to obtain the velocity dependence of the various non-linearities. Higher-order nonlinearities can be similarly constructed but are in fact irrelevant.

The noise-averaged correlations have the dynamic scaling form

$$\langle [h_\alpha(x,t) - h_\alpha(x',t')]^2 \rangle = |x - x'|^{2\chi_\alpha} f_\alpha \left(\frac{|x - x'|^{z_\alpha}}{|t - t'|} \right), \tag{4}$$

where f_α are scaling functions. This is easy to prove from Eqs. (1) in the absence of nonlinearities: The two independent diffusion equations can be solved to give $\chi_\parallel = \chi_\perp = \frac{1}{2}$ and $z_\parallel = z_\perp = 2$. The renormalization-group (RG) treatment indicates that all three nonlinear terms are relevant and may modify the exponents in Eq. (4). Recent studies of related stochastic equations [3,10] indicate that interesting dynamic phase diagrams may emerge from the competition between nonlinearities. Without loss of generality we assume that $\lambda_\parallel$ is positive and finite (its sign can be changed by $h_\parallel \to -h_\parallel$), and focus on the dependence of the scaling exponents on the ratios $\lambda_\perp/\lambda_\parallel$ and $\lambda_x/\lambda_\parallel$, as depicted in Fig. 2. (It is more convenient to set the vertical axis to $\lambda_x D_\perp \nu_\parallel / \lambda_\parallel D_\parallel \nu_\perp$.) Before pursuing the perturbative RG, we describe a number of nonperturbative properties of Eqs. (1).

Galilean invariance (GI).—Consider the infinitesimal reparametrization

$$x' = x + \lambda_\parallel \epsilon t, \quad t' = t, \tag{5}$$

$$h_\parallel' = h_\parallel + \epsilon x, \quad h_\perp' = h_\perp.$$

Equations (1) are invariant under this transformation provided that $\lambda_\parallel = \lambda_\perp$. Thus *along this line* in Fig. 2 there is GI, which implies the exponent identity [5,9] $\chi_\parallel + z_\parallel = 2$.

The Cole-Hopf (CH) transformation is an important method for the exact study of solutions of the one-component nonlinear diffusion equation [8]. Here we generalize this transformation to the complex plane by defining, for $\lambda_x < 0$,

$$\Psi(x,t) = \exp \left[\frac{\lambda_\parallel h_\parallel(x,t) + i(-\lambda_\parallel \lambda_x)^{1/2} h_\perp(x,t)}{2\nu} \right]. \tag{6}$$

The linear diffusion equation

$$\partial_t \Psi = \nu \partial_x^2 \Psi + \mu(x,t)\Psi \tag{7}$$

then leads to Eqs. (1) with $\nu_\parallel = \nu_\perp = \nu$ and $\lambda_\parallel = \lambda_\perp$. [Here $\mathrm{Re}(\mu) = \lambda_\parallel \eta_\parallel / 2\nu$ and $\mathrm{Im}(\mu) = (-\lambda_\parallel \lambda_x)^{1/2} \eta_\perp / 2\nu$.] This transformation enables an exact solution of the *deterministic* equation, and further allows us to write the solution to the *stochastic* equation in the form of a path integral

$$\Psi(x,t) = \int_{(0,0)}^{(x,t)} \mathcal{D}x(\tau) \exp \left\{ -\int_0^t d\tau \left[\frac{\dot{x}^2}{2\nu} + \mu(x,\tau) \right] \right\}. \tag{8}$$

Equation (8) has been extensively studied in connection with quantum tunneling in a disordered medium [11], with Ψ representing the wave function. In particular, results for the tunneling probability $|\Psi|^2$ suggest $z_\parallel = \frac{3}{2}$ and $\chi_\parallel = \frac{1}{2}$. The transverse fluctuations correspond to the phase in the quantum problem which is not an observable. Hence this mapping does not provide any information on $\chi_\perp$ and $z_\perp$ which are in fact observable for the moving line.

Fluctuation-dissipation (FD) condition.—The Langevin equations (1) lead to a Fokker-Planck equation for the evolution of the joint probability $\mathcal{P}[h_\parallel(x), h_\perp(x)]$. It can be shown that $\mathcal{P}$ has a stationary solution

$$\mathcal{P} = \exp \left[-\int dx \left[\frac{\nu_\parallel}{2D_\parallel} (\partial_x h_\parallel)^2 + \frac{\nu_\perp}{2D_\perp} (\partial_z h_\perp)^2 \right] \right], \tag{9}$$

provided that $\lambda_x \nu_\parallel D_\perp = \lambda_\perp \nu_\perp D_\parallel$. Thus for this special choice of parameters, depicted by a starred line in Fig. 2, if $\mathcal{P}$ converges to this solution, the long-time behavior of the correlation functions in Eq. (4) can be directly read off Eq. (9), giving $\chi_\parallel = \chi_\perp = \frac{1}{2}$.

At the point $\lambda_\perp = \lambda_x = 0$, $h_\parallel$ and $h_\perp$ decouple, and
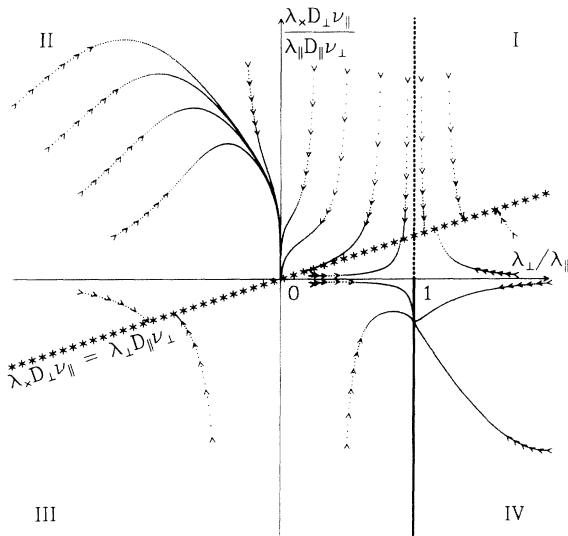

FIG. 2. Projected RG flows and the dynamic phase diagram. The conditions necessary for Galilean invariance, Cole-Hopf transformation, and fluctuation and dissipation are indicated by dotted, bold, and starred lines, respectively.

$z_\perp = 2$ while $z_\parallel = \frac{3}{2}$. However, in general, $z_\parallel = z_\perp = z$ unless the effective $\lambda_\perp$ is zero. For example, at the intersection of the subspaces with GI and FD the exponents $z_\parallel = z_\perp = \frac{3}{2}$ are obtained from the exponent identities. To construct the RG equations, we use only one value of z and check for consistency by requiring that $\lambda_\perp$ renormalizes to a finite value. The renormalization of the seven parameters in Eqs. (1) can be computed to one-loop order by standard methods of dynamic RG [5,9]. The recursion relations are straightforward, nevertheless too lengthy to reproduce here. Instead, the projections of the RG flows on the two-parameter subspace of Fig. 2 are indicated in this diagram. They naturally satisfy the constraints imposed by the nonperturbative results: the subspace of GI is closed under RG, while the FD condition appears as a *fixed line*. The RG flows have different behaviors in each quadrant of Fig. 2 as will be discussed in conjunction with the numerical results.

We also performed direct numerical integration of discretized versions of Eqs. (1). Similar simulations have explored the scaling properties of the interface growth equations [12]. We start from a flat initial condition, with periodic boundary conditions, and a lattice spacing taken as unity. The time step is chosen small enough to avoid short-distance instabilities, typically from 0.005 to 0.05. The spatial derivations are discretized symmetrically. At every step, the average motion of the line is subtracted to make $\bar{h}_a(t) = 0$. The average rms width can be calculated from Eq. (4), and has the dynamical scaling form $\langle w_a(t,L) \rangle = L^{\chi_a} f_a^w(L^{z_a}/t)$. Here L is the system size and the scaling functions f_a^w have the asymptotic behaviors $\lim_{u\to\infty} f_a^w(u) = A_a u^{-\chi_a/z_a}$ and $\lim_{u\to 0} f_a^w(u) = B_a$, with A_a, B_a being constants. Therefore, the large t, i.e., steady-state, behavior of w_a scales as L^{χ_a}, whereas the large L, small t behavior is t^{β_a}, with $\beta_a = \chi_a/z_a$. For the large t analysis, the steady-state rms width is measured for system sizes $L = 16, 32, 64, 128,$ and 256. For the dynamic analysis, system width is measured as a function of

time for $L = 60000$, up to $t = 300$. Numerical integrations were performed for different sets of parameters in Eqs. (1), and the exponents obtained by the above procedure are indicated in Table I. Not all exponents correspond to their true asymptotic values.

The scaling behavior for the different regions in Fig. 2, obtained by combining nonperturbative, RG, and numerical results, is summarized below.

$\lambda_\perp \lambda_x > 0$: Our conclusions in these regions are the most reliable. The RG flows terminate on the fixed line where FD conditions apply, hence $\chi_\parallel = \chi_\perp = \frac{1}{2}$. All along this line, the one-loop RG exponent is $z = \frac{3}{2}$. These results are consistent with the numerical simulations. The measured exponents rapidly converge to these values, except when $\lambda_\perp$ or λ_x are small.

$\lambda_x = 0$: In this case the equation for $h_\parallel$ is identical to that of an interface in $1+1$ dimensions, and $\chi_\parallel = \frac{1}{2}$, with $z_\parallel = \frac{3}{2}$. The fluctuations in $h_\parallel$ act as a strong (multiplicative and correlated) noise on $h_\perp$. The one-loop RG yields the exponents $z_\perp = \frac{3}{2}$, $\chi_\perp = 0.75$ for $\lambda_\perp > 0$, while a negative $\lambda_\perp$ scales to 0 suggesting $z_\perp > z_\parallel$. Simulations are consistent with the RG calculations for $\lambda_\perp > 0$, yielding $\chi_\perp = 0.72$, surprisingly close to the one-loop RG value. If one considers the mapping $-\partial_x h_\parallel \mapsto \mathbf{V}$, Eqs. (1) (for $\lambda_x = 0$ *and* $\lambda_\perp > 0$) describe convection of a passive scalar $h_\perp$, e.g., temperature if we set $h_\perp$ to T, by a velocity field $\mathbf{V}$ [9]. The RG flows in Fig. 2 assure GI in the hydrodynamic limit *even if* $\lambda_\perp \neq \lambda_\parallel$ *initially*. Furthermore, our analysis indicates that a nonconserved noise acting on T is relevant and increases the exponent χ_T of thermal fluctuations ($\langle [T(x) - T(x')]^2 \rangle \propto |x - x'|^{2\chi_T}$), at least for $d = 1$. For $\lambda_\perp < 0$, simulations indicate $z_\perp \approx 2$ and $\chi_\perp \approx \frac{2}{3}$ along with the expected values for the longitudinal exponents.

$\lambda_\perp = 0$: The transverse fluctuations satisfy a simple diffusion equation with $\chi_\perp = \frac{1}{2}$ and $z_\perp = 2$. Through the term $\lambda_x (\partial_x h_\perp)^2/2$, these fluctuations act as a corrected noise [5] for the longitudinal mode. A naive application

TABLE I. Numerical estimates of the exponents for various values of model parameters. In all runs, $v_\parallel = v_\perp = 1$ and $D_\parallel = D_\perp = 0.01$, unless indicated otherwise. Values for z are calculated from the ratio of the previous two entries.

Quadrant[a]	$\chi_\parallel$	$\beta_\parallel$	$z_\parallel$	$\chi_\perp$	$\beta_\perp$	$z_\perp$	$\lambda_\parallel$	λ_x	$\lambda_\perp$
I	0.48	0.33	1.46	0.48	0.33	1.46	20	20	20
I	0.75	0.58	1.29	0.50	0.27	1.85	20	20	2.5
I	0.51	0.29	1.76	0.56	0.35	1.60	20	5	25
II [b]	0.83	Unstable		0.44	0.28	1.57	5	5	-5
III	0.50	0.32	1.56	0.50	0.34	1.47	20	-20	-20
IV [b]	0.52	0.30	1.73	0.57	0.29	1.97	5	-5	5
I-IV boundary	0.49	0.32	1.53	0.72	0.46	1.57	20	0	20
II-III boundary	0.48	0.33	1.46	0.65	0.32	2.03	20	0	-20
I-II boundary	0.84 [c]	0.71	1.18	0.50	0.25	2.00	20	20	0
III-IV boundary	0.55	0.34	1.62	0.51	0.25	2.04	20	-20	0

[a]See Fig. 2.
[b]Roughening exponents measured from height-height correlations, for $D_a = 0.002$.
[c]This exponent increases with system size, suggesting nonscaling behavior.

of the results in Ref. [5] gives $\chi_\| = \frac{2}{3}$ and $z_\| = \frac{4}{3}$. Quite surprisingly, simulations indicate different behavior depending on the sign of λ_x. For $\lambda_x < 0$, $z_\| \approx \frac{3}{2}$ and $\chi_\| \approx \frac{1}{2}$, whereas for $\lambda_x > 0$, longitudinal fluctuations are much stronger, resulting in $z_\| \approx 1.18$ and $\chi_\| \approx 0.84$. Actually, $\chi_\|$ increases steadily with system size, suggesting a breakdown of dynamic scaling, due to a change of sign in $\lambda_\perp\lambda_x$. This dependence on the sign of λ_x may reflect the fundamental difference between behavior in quadrants II and IV of Fig. 2. A number of recent experiments, from immiscible displacement in porous media [13,14] to evolution of bacterial colonies [15], observe interfaces in 1+1 dimensions with a roughness exponent near 0.8. Various other fields (e.g., fluid pressure, nutrient concentration) are certainly present in such experiments. The above example indicates that coupling to such fields may indeed lead to larger roughness exponents [16].

$\lambda_\perp < 0$ *and* $\lambda_x > 0$: The analysis of this region (II) is the most difficult in that the RG flows do not converge upon a finite fixed point *and* $\lambda_\perp \to 0$, which may signal the breakdown of dynamic scaling. Simulations indicate strong longitudinal fluctuations that lead to instabilities in the integration scheme, making it impossible to measure exponents by the described method. The equal-time height-height correlations in Eq. (4) can still be used to determine effective roughening exponents at small nonlinearity, disorder, and system size, but the results are not as accurate or reliable.

$\lambda_\perp > 0$ *and* $\lambda_x < 0$: The *projected* RG flows in this quadrant (IV) converge to the point $\lambda_\perp/\lambda_\| = 1$ and $\lambda_x D_\perp v_\|/\lambda_\| D_\| v_\perp = -1$. This is actually not a fixed point, as $D_\|$ and $D_\perp$ scale to infinity. The applicability of the CH transformation to this point implies $z_\| = \frac{3}{2}$ and $\chi_\| = \frac{1}{2}$. Since $\lambda_\perp$ is finite, we expect $z_\perp = z_\| = \frac{3}{2}$, but we have no information on $\chi_\perp$. Simulations indicate strong transverse fluctuations and roughening exponents are again obtained from height-height fluctuations instead. Dynamical exponents had to be read off at relatively earlier times and are not reliable enough to be conclusive.

In conclusion, we have introduced the simplest nonlinear, local, and dissipative equations that govern the fluctuations of a moving line in a random medium. By a combination of exact results, perturbative RG, and numerical simulations, we conclude that in most cases the relaxation of fluctuations is superdiffusive with an exponent $z = \frac{3}{2}$. Special choices of parameters lead to decoupling of transverse and longitudinal fluctuations, and enhancement of roughness exponents. The presented approach is easily generalized to describe evolution of a manifold with arbitrary internal ($\mathbf{x} \in R^d$) and external ($\mathbf{h} \in R^n$) dimensions, and to the motion of curves that are not necessarily stretched in a particular direction [17]. However, in contrast to Ref. [17], the evolution Eqs. (1) do not have intrinsic reparametrization invariance or local arclength conservation. Thus, the motion of a string (with no line tension) may be subject to additional symmetries. Details of the calculations, and such generalizations, are left to future publications. There are by now many simulations and experiments on the dynamic roughening of growing interfaces, explained by such nonlinear evolution [1]. It would be very interesting if similar realizations can be found for the dynamics of moving lines. Possibilities include electrophoresis of a charged linear polymer, or driven line dislocations in a liquid crystal, in addition to the driven magnetic flux line explicitly discussed. We should, however, emphasize that for each of these examples the assumptions regarding the locality of interactions and short-range nature of noise correlations need to be carefully examined. Equations (1) thus provide a *starting framework* for studying these problems.

[1] See, e.g., *Dynamics of Fractal Surfaces*, edited by F. Family and T. Vicsek (World Scientific, Singapore, 1991).

[2] M. Kardar, in *Disorder and Fracture*, edited by J. C. Charmet, S. Roux, and E. Guyon (Plenum, New York, 1990); T. Hwa and M. Kardar, Phys. Rev. A **45**, 7002 (1992).

[3] T. Hwa (private communication).

[4] M. Plischke, Z. Rácz, and D. Liu, Phys. Rev. B **35**, 3485 (1987).

[5] E. Medina, T. Hwa, M. Kardar, and Y. Zhang, Phys. Rev. A **39**, 3053 (1989).

[6] Y.-C. Zhang, J. Phys. (Paris) **51**, 2129 (1990).

[7] M. Kardar, G. Parisi, and Y. Zhang, Phys. Rev. Lett. **56**, 889 (1986).

[8] J. M. Burgers, *The Nonlinear Diffusion Equation* (Riedel, Boston, 1974).

[9] D. Forster, D. R. Nelson, and M. J. Stephen, Phys. Rev. A **16**, 732 (1977).

[10] D. Wolf, Phys. Rev. Lett. **67**, 1783 (1991).

[11] E. Medina, M. Kardar, Y. Shapir, and X.-R. Wang, Phys. Rev. Lett. **62**, 941 (1989); E. Medina and M. Kardar, Phys. Rev. B (to be published).

[12] J. G. Amar and F. Family, Phys. Rev. A **41**, 3399 (1990); B. Grossman, H. Guo, and M. Grant, Phys. Rev. A **43**, 1727 (1991).

[13] M. A. Rubio, C. A. Edwards, A. Dougherty, and J. P. Gollub, Phys. Rev. Lett. **63**, 1685 (1989).

[14] V. K. Horváth, F. Family, and T. Vicsek, Phys. Rev. Lett. **67**, 3207 (1991).

[15] T. Vicsek, M. Cserzö, and V. K. Horváth, Physica (Amsterdam) **167A**, 315 (1990).

[16] For other possible explanations, see Ref. [6]; D. Kessler, H. Levine, and Y. Tu, Phys. Rev. A **43**, 4551 (1991).

[17] R. E. Goldstein and D. M. Petrich, Phys. Rev. Lett. **67**, 3203 (1991); S. A. Langer and R. E. Goldstein (to be published).